1990ApJ...365..686M

THE ASTROPHYSICAL JOURNAL, 365:686–695, 1990 December 20
© 1990. The American Astronomical Society. All rights reserved. Printed in U.S.A.

MS 1603.6+2600, AN UNUSUAL X-RAY SELECTED BINARY SYSTEM AT HIGH GALACTIC LATITUDE[1,2]

SIMON L. MORRIS AND JAMES LIEBERT[3]
Observatories of the Carnegie Institution of Washington

JOHN T. STOCKE
CASA, University of Colorado

AND

ISABELLA M. GIOIA,[4] RUDY E. SCHILD, AND ANNA WOLTER
Harvard-Smithsonian Center for Astrophysics
Received 1990 February 20; accepted 1990 June 21

ABSTRACT

We describe the discovery of an eclipsing binary system at Galactic latitude 47°, found as a serendipitous X-ray source in the *Einstein* Extended Medium Sensitivity Survey. The object has X-ray flux 1.1×10^{-12} ergs cm^{-2} s^{-1} (0.3–3.5 keV) and mean magnitude $R \sim 19.4$. An orbital period of 111 minutes is found. We discuss whether the system has a white dwarf or neutron star primary, in the end preferring the neutron star primary model. If the system has either optical or X-ray luminosities typical of low mass X-ray binaries (LMXB), it must be at a very large distance (30–80 kpc). Blueshifted He I absorption is seen, indicating cool outflowing material, similar to that seen in the LMXB AC 211 in the globular cluster M15.

Subject headings: stars: eclipsing binaries — stars: individual (MS 1603.6+2600) — X-rays: binaries

I. INTRODUCTION

MS 1603.6+2600 is an X-ray source in the *Einstein Observatory* Extended Medium Sensitivity Survey (EMSS, Gioia *et al.* 1990). This survey contains the 835 serendipitous sources with statistical significance $\geq 4\ \sigma$ found in *Einstein* IPC images with $b(\mathrm{II}) > 20°$. The EMSS is thus a flux-limited and homogeneous sample of high Galactic latitude X-ray sources. An optical identification program is approximately 90% complete, with ~74% of the identifications being extragalactic. Of the Galactic objects, the majority are late-type main-sequence stars with coronal emission (Fleming, Gioia, and Maccacaro 1989). Excluding MS 1603.6+2600, there are currently five cataclysmic variables in the EMSS, including two AM Herculis systems (Morris *et al.* 1987) and no X-ray binaries.

The error circle for MS 1603.6+2600 contained three candidate objects visible on the sky survey. The brightest (to the northwest of the X-ray centroid) was found to be a normal star. A fainter candidate to the south of the centroid was also found to be a star. The candidate northeast of the centroid was initially classified as a possible BL Lacertae–type active galaxy, based on its nearly featureless optical spectrum and high X-ray to optical flux ratio [$\log (f_x/f_v) = 1.2$, see Maccacaro *et al.* 1988 for definition]. However, VLA observations placed a very low upper limit on the radio flux from this object, giving a radio-to-optical flux ratio well below that of typical EMSS BL Lac objects ($\alpha_{ro} < 0.15$, Stocke *et al.* 1990*a*). Further optical spectroscopy and photometry show that this object is some kind of short-period Galactic binary system with very low equivalent width emission lines, either an unusual type of cataclysmic variable (CV) or a low mass X-ray binary (LMXB). An accurate optical position for MS 1603.6+2600 is R.A. $16^h3^m40^s.50$; decl. $+25°59^m48^s.1$ (1950), which corresponds to Galactic coordinates l(II) 42°.8; b(II) 46°.8. A finding chart for this object will be published in Stocke *et al.* (1990*b*).

In § II below, we describe the observations of this object, and in § III the analysis of the observations. We then discuss some of the possible models for MS 1603.6+2600 in § IV, summarizing our conclusions in § V.

II. OBSERVATIONS

a) X-Ray Observations

MS 1603.6+2600 was discovered as a serendipitous source in IPC field 4607 (centered on Mrk 495) during a 2112 s exposure. Fifty-one counts were recorded; insufficient to analyze either for variability or detailed spectral shape. Assuming a thermal spectrum (Raymond and Smith 1977) with temperature in the range 8×10^5 to 3×10^6 K, and no correction for hydrogen column density along the line of sight, this corresponds to a flux of 1.14×10^{-12} ergs cm^{-2} s^{-1} in the 0.3–3.5 keV energy band, which in turn implies a luminosity of 1.4×10^{34} $(d/10\ \mathrm{kpc})^2$ ergs s^{-1}. Note that the hardness ratio for this object (see Maccacaro *et al.* 1988 for details on this parameter and its interpretation) is 0.58 ± 0.12, which suggests either a very hard X-ray spectrum or a large absorbing column. See Gioia *et al.* (1990) for a more complete description of the X-ray analysis.

b) Optical Photometry

A summary of all the optical observations (photometric and spectroscopic) taken to date is given in Table 1.

MS 1603.6+2600 was observed with the Mount Hopkins 24 inch (61 cm) telescope over the period 1987 March to 1988 May on a total of 53 separate nights. At the time of the obser-

[1] This paper uses data obtained at the Multiple Mirror Telescope Observatory (MMTO), which is operated jointly by the University of Arizona and the Smithsonian Institution.

[2] Observations were partially made at Palomar Observatory as part of a collaborative agreement between the California Institute of Technology and the Carnegie Institution of Washington.

[3] Permanent address: Steward Observatory, University of Arizona, Tucson, AZ 85721.

[4] Also from Instituto di Radioastronomia del CNR, Bologna, Italy.

© American Astronomical Society • Provided by the NASA Astrophysics Data System

1990ApJ...365..686M

TABLE 1

TABLE OF OPTICAL OBSERVATIONS

Telescope	Date	Description
MMT	1988 Mar 20	Optical spectroscopy
Mount Hopkins 24 inch ...	1987 Mar–1988 Mar	Optical photometry
Palomar 200 inch	1988 Aug 10	Optical spectroscopy
Palomar 60 inch	1989 May 23–26	Differential optical photometry
Palomar 200 inch	1989 Jun 27–28	Optical spectroscopy

vations the nature of MS 1603.6+2600 was still uncertain, and so no attempt was made to obtain a continuous sequence of observations with high time resolution. Also, due to the faintness of the object, a minimum exposure time of 20 minutes was required. From this data base, a mean Johnson *R* magnitude of 19.42 was derived with maximum and minimum magnitudes of 18.87 and 20.10 (although bear in mind that these magnitudes are all averages over the 20 minute exposure period). This photometry showed no excursions outside of the fairly narrow range 18.9–20.1, and no long-term trends on time scales of weeks. (See § III*a*) for a description of systematic changes on shorter time scales).

MS 1603.6+2600 was also observed at the Palomar 60 inch (1.5 m) telescope with a TI CCD and reimaging optics. It was monitored in white light (no filter) for four nights (1989 May 23–26). Exposure times were 5 minutes, with gaps between exposures of 1 minute for CCD readout and preparation. A total of 188 exposures were obtained. The first night was plagued by thin clouds, but the remaining three nights were photometric.

Aperture photometry of MS 1603.6+2600 and also the two nearby stars was performed using the IRAF APPHOT package.[5]

Because of color differences, the two stars and also MS 1603.6+2600 showed different dependence of magnitude on airmass. For the two stars, a straight line fit to a plot of magnitude versus airmass gave the extinction coefficients, which were then used to make the extinction correction. In the case of MS 1603.6+2600, this procedure was complicated by the intrinsic variability of the object. However, an approximate extinction coefficient was derived, using the data from the last night only, by fitting to the upper envelope of the magnitude versus airmass plot. Because of the nonphotometric conditions on the first night, only the magnitude differences between MS 1603.6+2600 and the stars in the field are considered. The magnitude differences between MS 1603.6+2600 and the brighter star in the field are plotted as a function of time in Figure 1. Error bars show the estimated 1 σ error based on photon statistics. The magnitude difference between the two stars had a mean of 0.491 and rms of 0.050, consistent with the photon statistics, and showed no systematic trends, and so only the comparison between MS 1603.6+2600 and the brighter star will be considered.

c) *Optical Spectroscopy*

MS 1603.6+2600 was first observed spectroscopically at the MMT on 1988 March 20 with the MMT spectrograph and an intensified Reticon detector. A 300 line mm^{-1} grating was used, giving a resolution of ~ 7 Å (FWHM). No firm identifica-

[5] IRAF is distributed by NOAO, which is operated by AURA, Inc., under contract to the NSF.

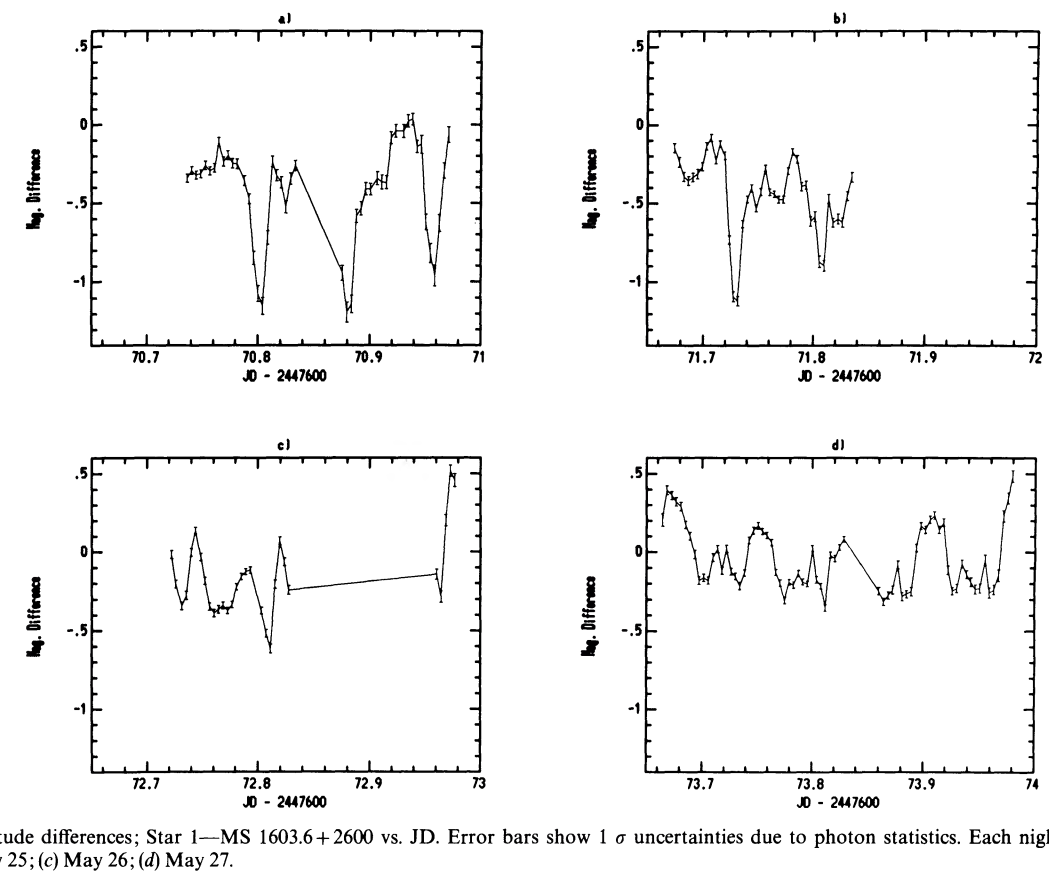

FIG. 1.—Magnitude differences; Star 1—MS 1603.6+2600 vs. JD. Error bars show 1 σ uncertainties due to photon statistics. Each night plotted separately. (*a*) May 24; (*b*) May 25; (*c*) May 26; (*d*) May 27.

© American Astronomical Society • Provided by the NASA Astrophysics Data System

1990ApJ...365..686M

tion was obtained from this spectrum, although a preliminary classification as a BL Lac candidate was made, based on its blue color, weak or absent emission lines and high X-ray to optical flux ratio (F_x/F_{opt}).

Further spectroscopic observations were obtained at the Palomar 200 inch (5.1 m) on 1988 August 10 at 4.78 UT. The double spectrograph was used with a resolution of $\sim$6.5 Å of the blue side and $\sim$18 Å on the red side. Two half-hour exposures were obtained, which were enough to detect the He II and Hα emission lines near rest, and hence classify the object as a Galactic binary system.

One month after the Palomar 1.5 m photometry run described in § II*b* above, two more nights of spectroscopic data were obtained on the Palomar 5.1 m (1989 June 27–28). On the first night, the same low-resolution gratings were used as above. On the second night, the gratings were changed to give resolutions of 1.7 Å and 2.5 Å in the blue and red respectively, and coverage from 4560 to 5006 Å and 6235 to 6889 Å. A total of 13 15 min exposures were obtained at low dispersion, and 15 15 minute exposures at high dispersion.

The means of the 13 flux-calibrated low-resolution spectra in the blue and red for MS 1603.6+2600 are shown in Figures 2*a* and *b*. The high-dispersion Palomar data were left in extinction corrected counts per integration time (1 count = 1.5 electrons in the blue and 2.0 electrons in the red). The summed counts from all 15 high-dispersion observations are shown in Figures 3*a* and *b*, smoothed by a boxcar of width 8.5 and 12.5 Å, respectively.

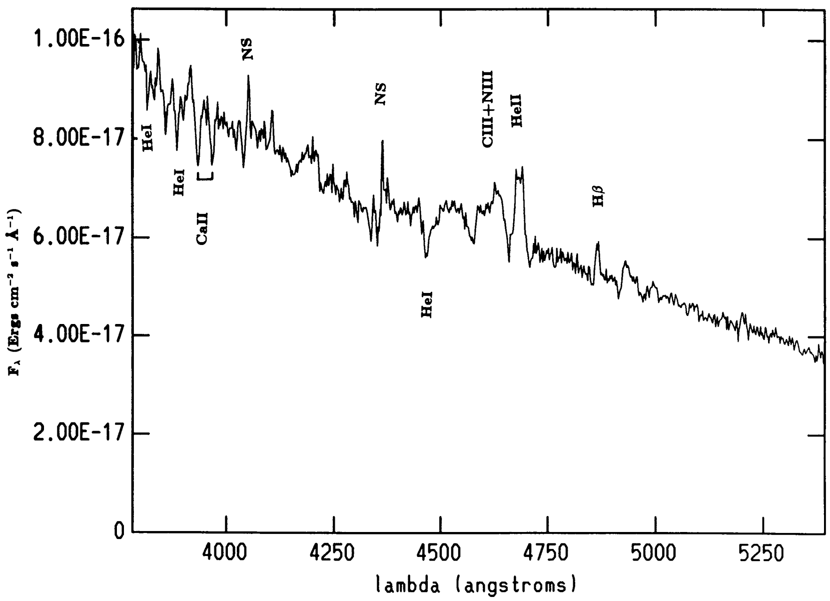

FIG. 2*a*

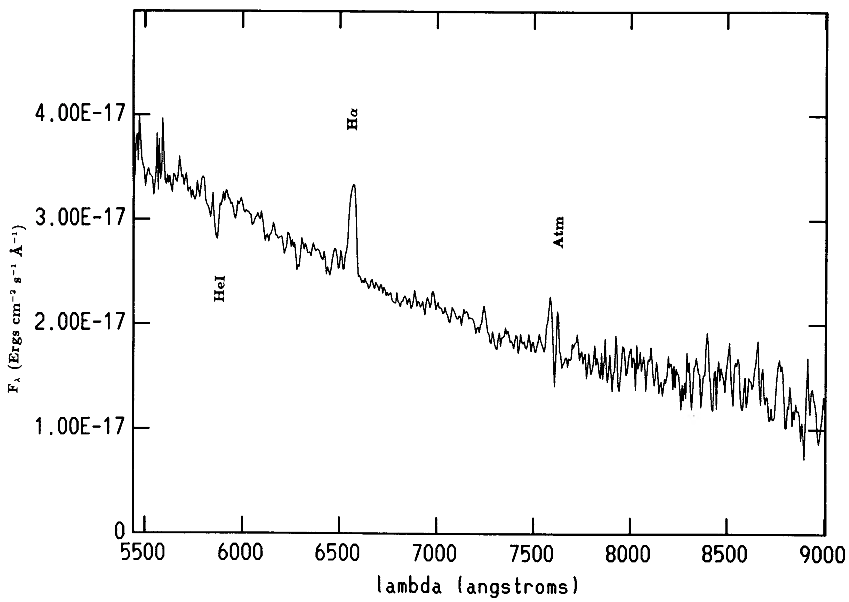

FIG. 2*b*

FIG. 2.—(*a*) Mean blue low-resolution spectrum of MS 1603.6+2600; (*b*) Mean red low-resolution spectrum. Line strengths and wavelengths are given in Table 3.

© American Astronomical Society • Provided by the NASA Astrophysics Data System

1990ApJ...365..686M

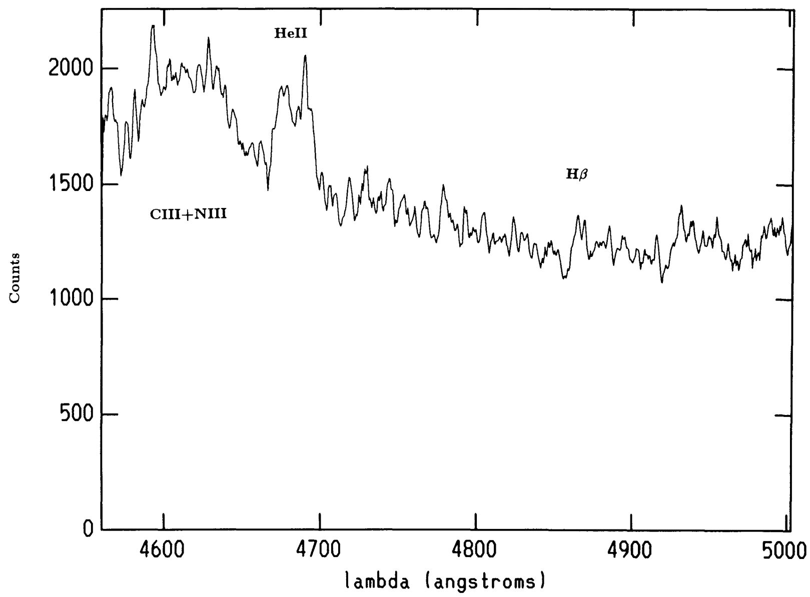

FIG. 3a

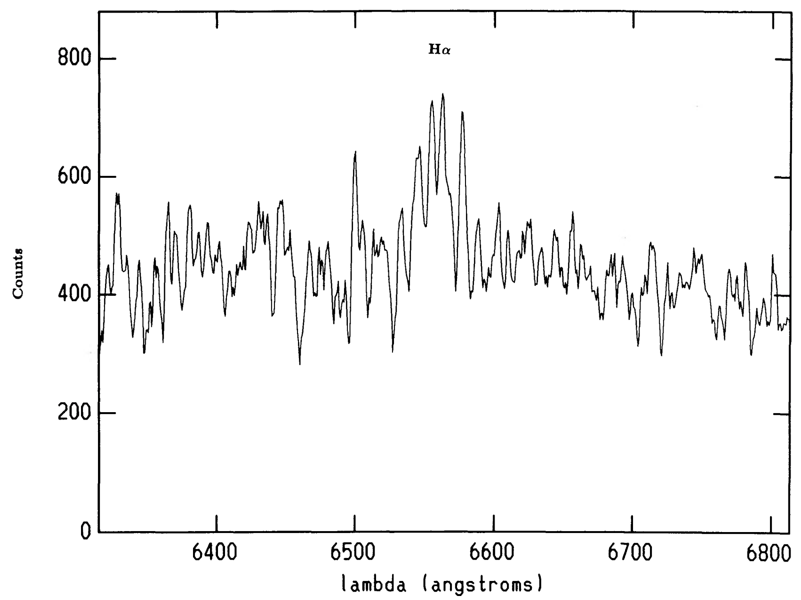

FIG. 3b

FIG. 3.—(*a*) Summed blue high-resolution spectrum; (*b*) Summed red high-resolution spectrum. *Y*-axis is CCD counts where for (*a*) 1 count = 1.5 electrons and for (*b*) 1 count = 2 electrons. The data have been smoothed with a boxcar (see text).

d) *Radio Data*

Observations of MS 1603.6+2600 were obtained on 1987 October 24 at 6 cm in "snapshot mode" with the VLA in A/B configuration. Fifty-five minutes of data were obtained at frequencies 4835 and 4885 MHz with bandwidths of 50 MHz. Flux calibration was made assuming flux densities of 5.36 Jy for 3C 48 and 7.41 Jy for 3C 286 (Baars *et al.* 1977). From these data, a 5 σ upper limit of less than 0.3 mJy can be placed on any source at the optical position.

e) *Polarimetry*

MS 1603.6+2600 was observed by Buell Jannuzi (private communication) on two occasions with the Two-Holer photometer/polarimeter on the Steward Observatory 90 inch (2.3 m) telescope in white light. Upper limits on the linear polarization obtained were less than 5% on 1988 June 6, and less than 4.5% on 1988 October 8.

III. ANALYSIS

a) *The Optical Photometry*

It can be seen from Figure 1 that during the four nights of monitoring MS 1603.6+2600 gradually brightened. During the first night, clear sharp eclipses occurred. As the object brightened, the eclipses weakened, until by the fourth night they have more or less disappeared. In fact local minima can be identified for 10 eclipses during the four nights. Fitting a parabola to the photometry at each minimum gives the eclipse times in Table 2. At least-squares fit to these times with an

© American Astronomical Society • Provided by the NASA Astrophysics Data System

TABLE 2

TABLE OF ECLIPSE TIMES

Orbit Number	JD
1	2,447,670.8031
2	2,447,670.8817
3	2,447,670.9582
13	2,447,671.7297
14	2,447,671.8078
26	2,447,672.7313
27	2,447,672.8101
29	2,447,672.9637
39	2,447,673.7336
40	2,447,673.8114

assumed error of 2 minutes for each eclipse gives an ephemeris (with phase zero defined as the bottom of the eclipse) of

$$\text{JD at eclipse} = 2{,}447{,}670.72709(\pm 0.00075) + N \times 0.077108(\pm 0.000029) \text{ days ,}$$

i.e., a period of 111.04 minutes is found. With the above ephemeris, the photometry can be phased. Figure 4 shows the phased photometry, with each night plotted separately to show the steady change in the light curve. For clarity error bars have been left off, but as the y-scale is the same as Figure 1, it is straightforward to transfer typical errors. The eclipse can be seen to be initially quite sharp, covering about a quarter of the orbit, and about 0.8 magnitudes deep during the first night. By the final night, the eclipse has nearly vanished, and a broad hump between phase 0.1 and 0.4 appears.

b) The Optical Spectroscopy

i) *Phasing the Spectroscopy*

Unfortunately the ephemeris determined from the four nights of photometry was not accurate enough to be useful at the time of the later spectroscopy. In order to phase the low-resolution spectroscopy, the mean flux in 500 Å bands in the low-resolution data was measured (4000–4500 Å, 4750–5250 Å, 6000–6500 Å, 7000–7500 Å and 8000–8500 Å). A plot of these fluxes versus Julian Day is shown in Figure 5a. An eclipse is seen at JD 2,447,705.79, and is assigned phase zero. This phasing matches with local minima in the mean counts in the high-dispersion spectra of the second night. The one month separation between the differential photometry and the spectroscopy is too long to allow determination of the "orbit number" of this eclipse, and hence an improvement in the orbital period. Figure 5b shows the variation in flux ratio between the various low-resolution bins. As can be seen, there is a systematic trend toward lower fluxes and redder colors through the night which seems to dominate any phase-dependent color variations.

ii) *Low Resolution*

In order to estimate the wavelength errors in the low-resolution data, data extraction was repeated without sky subtraction. This gave several strong sky lines extracted from the same (optimal) aperture as the data. Measurement of these lines gave zero point shifts of 0.04 Å (with rms 0.07 Å) for the blue side and −1.3 Å (with rms 0.42 Å) for the red side. The wavelength scales were thus shifted by this amount. The rms values can be considered to be the minimum 1 σ errors in the low-resolution wavelengths for a strong sharp line.

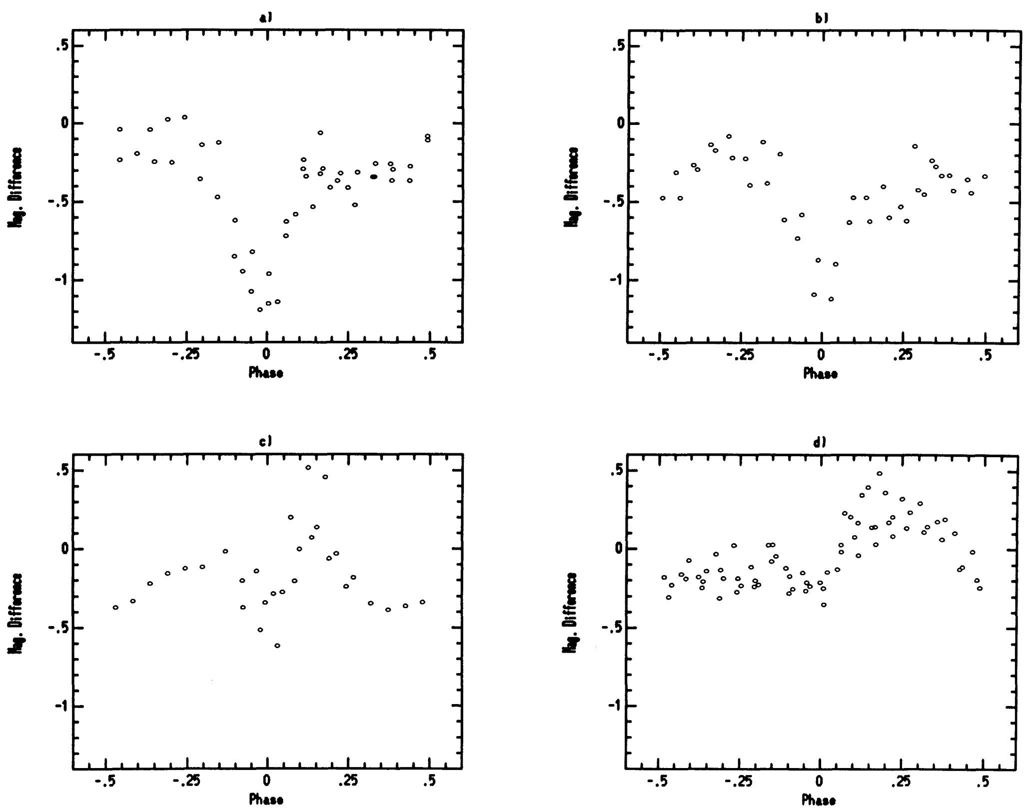

FIG. 4.—Magnitude differences; Star 1—MS 1603.6+2600 vs. phase. As for Fig. 1, the nights are plotted separately. (a) May 24; (b) May 25; (c) May 26; (d) May 27.

© American Astronomical Society • Provided by the NASA Astrophysics Data System

1990ApJ...365..686M

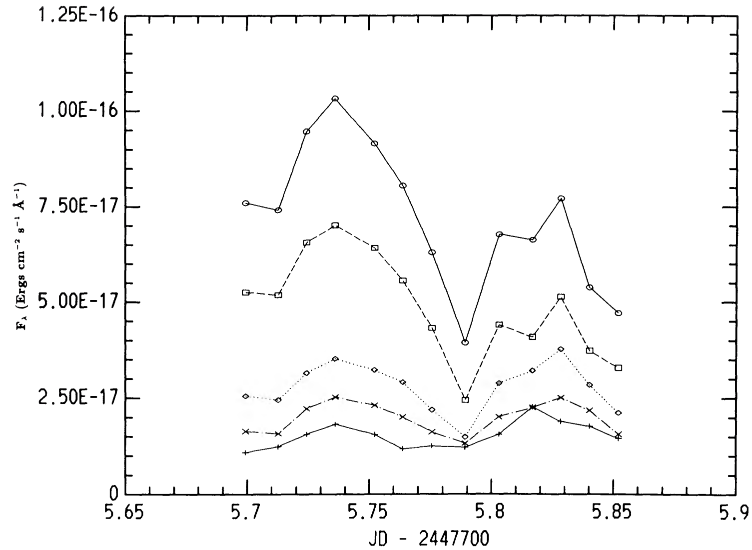

FIG. 5*a*

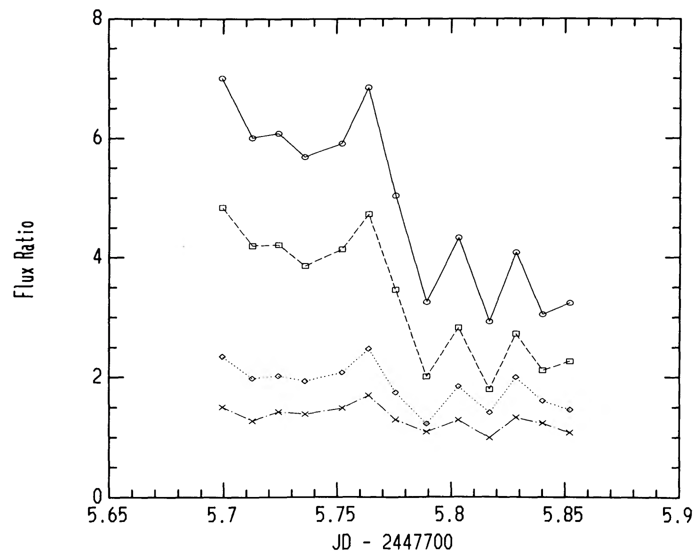

FIG. 5*d*

FIG. 5.—(*a*) Continuum fluxes in 500 Å bins vs. JD from the low-resolution spectroscopy. *Solid line + circles*: 4000–4500 Å; *dashed line + boxes*: 4750–5250 Å; *dotted line + diamonds*: 6000–6500 Å; *dot-dash line + crosses*: 7000–7500 Å; *solid line + pluses*: 8000–8500 Å. (*b*) Continuum flux-ratios vs. JD. *Solid line + circles*: 4000–4500 Å/8000–8500 Å; *dashed line + boxes*: 4750–5250 Å/8000–8500 Å; *dotted line + diamonds*: 6000–6500 Å/8000–8500 Å; *dot-dash line + crosses*: 7000–7500 Å/ 8000–8500 Å.

Emission and absorption line centroids and equivalent widths (EW) were measured interactively using a subjectively determined local straight line fit to the continuum. These numbers and the line identifications for the mean spectrum shown in Figure 2*a* and *b* are included in Table 3. Wavelength errors for weak or broad features could be as large as 1 Å. The flux and equivalent width errors are dominated by uncertainty in the local continuum value and are approximately a factor of 2 for features with EW < 1.0 Å and a factor 1.3 for stronger features. The heliocentric velocities of various ions and lines from these data are included as Table 4. Errors for these values are ± 50 km s^{-1} except for Hβ which has a larger uncertainty of ± 100 km s^{-1} due to its weakness.

Only the He II $\lambda 4686$ and Hα emission lines were strong enough to measure in the individual spectra. The observation JD and phase, line centroids and EWs are given in Table 5. For entries *not* marked with a colon estimated errors are ± 0.5 Å for He II and ± 1 Å for Hα and a factor of 1.5 in the EWs. Entries marked with a colon are considerably less reliable due to either low S/N or unfortunate placement of a cosmic-ray event. For nine of the 13 low-resolution observations the He I absorption line at 4471 Å could be seen, and these measurements are included in Table 5. Due to the weakness of the line, the He I wavelengths are uncertain by 1 Å and the EWs by a factor of 2. It can be seen that the He II and Hα emission line EWs rise during the eclipse at JD 2,447,705.79. This indicates that neither the He II nor the Hα fluxes are significantly reduced in this eclipse. The He I lines are systematically shifted blueward of the emission lines, but their behavior as a function of phase cannot be determined with our data. The emission-

© American Astronomical Society • Provided by the NASA Astrophysics Data System

1990ApJ...365..686M

TABLE 3

TABLE OF LOW-RESOLUTION SPECTROSCOPIC RESULTS

λ (Å)	Flux[a]	EW[b] (Å)	ID[c]
3816.4	−4.23E-17	−0.452	He I 3819.607
3841.9:.........	3.65E-17:	0.403:	?
3858.3	−3.00E-17	−0.342	?
3884.2	−3.27E-17	−0.383	He I 3888.65
3914.7:.........	9.53E-17:	1.11:	?
3933.0	−8.88E-17	−1.05	Ca II 3933.66
3966.7	−7.27E-17	−0.868	Ca II 3968.47
4105.4	5.66E-17	0.725	Hδ?
4194.8	2.80E-16	3.92	Blend
4335.5:.........	−4.32E-17:	−0.660:	Hγ?
4466.9	−6.44E-17	−1.03	He I 4471.479
4524.8:.........	2.56E-16:	4.12:	Blend
4621.5	3.92E-16	6.42	Blend
4660.0:.........	−2.39E-17:	−0.394:	?
4684.4	3.61E-16	6.18	He II 4685.7
4866.7	7.43E-17	1.43	Hβ
4938.2	1.31E-16	2.65	Blend
5202.3:.........	2.70E-17:	0.649:	Blend
5408.8:.........	1.30E-16:	3.70:	Blend
5867.4	−1.04E-16	−3.28	He I 5875.62
6563.5	3.63E-16	14.6	Hα
7245.5:.........	5.11E-17:	2.67:	?

NOTES.—Values followed by a colon are very uncertain.

[a] Flux in ergs cm^{-2} s^{-1} Å^{-1}. Negative values indicate absorption lines.

[b] N.B.: For consistency with the flux column, and counter to the usual convention, negative EWs indicate absorption lines.

[c] " ? " entries in the ID column indicate no ID (often the line's existence is questionable); " Blend " entries also indicates no ID, and that the feature is broader than expected for a single line.

TABLE 4

TABLE OF LOW-RESOLUTION ION AND LINE VELOCITIES

Ion/Line	Velocity (helio.)[1] km s^{-1}
He I absent	−314
Ca II absent	−84
He II	−77
Hβ	339
Hα	68

[1] See text for a discussion of the errors in these values.

line velocity as a function of phase is poorly determined by our data and further observations are needed.

The observed mean R magnitude can be converted to a V magnitude (for comparison with other classes of objects in the literature) using the spectral shape derived from the low-resolution spectra. These spectra give a $V-R$ color of 0.29, indicating a mean V magnitude of 19.73.

iii) *High Resolution*

In order to establish the zero point for the high-dispersion observations, two observations of the twilight sky and four observations of radial velocity standard stars from Peterson, Olszewski, and Aaronson (1986) were obtained. Measurement of the Hβ and Hα absorption features in these observations gave a zero point offset for the high-dispersion data of −1.3 (with rms 2.3) km s^{-1} for the blue and 1.3 (with rms 4.5) km s^{-1} for the red. These offsets are negligible given the uncertainty in the profile measurements and have not been included in the velocities quoted below. The S/N in the individual high-dispersion spectra are not sufficient to measure line properties as a function of orbital phase. Measurements of the summed spectra yield centroid radial velocities for the He II emission line of -82 ± 50 km s^{-1} (heliocentric) and -227 ± 200 km s^{-1} (heliocentric) for the (marginally detected) Hα line. The large uncertainties in the line velocities are entirely due to the complex profile and the faintness of the object. The He II profile is well resolved (FWZI of 2000 km s^{-1}) and shows a square topped shape, with a sharp spike at radial velocity +263 km s^{-1} (heliocentric) (see Fig. 3*a*).

IV. DISCUSSION

The observations presented here require that MS 1603.6+2600 be modeled as an accreting, close binary system whose primary is a compact object. The derived orbital period of just less than 2 hr implies that the mass donor is less than $\sim 0.2\ R_\odot$, the Roche lobe radius for a low-mass companion at this period. (N.B.: The Roche lobe size is a function of the mass ratio of the two components; see Pringle 1985 for a convenient plot.) This size corresponds to a cool main-sequence star of very low mass, i.e., $\lesssim 0.2\ M_\odot$. Note, however, that evolved subdwarf O or B stars may also be roughly this size and such objects are more massive. Nevertheless, the changing light curve makes it reasonable to assume that the optical continuum and emission lines are emitted by an accretion disk

TABLE 5

TABLE OF TIME-RESOLVED LOW-RESOLUTION SPECTROSCOPY

JD	Phase	He II λ (Å)	He II EW (Å)	Hα λ (Å)	Hα EW (Å)	He I λ (Å)	He I EW (Å)
2,447,705.6994.........	0.8355	4683.5	7.2	6565.9	12.1	4465.4	3.2
2,447,705.7127.........	0.0087	4683.0	5.4	6558.6	21.2	4465.1:	1.2:
2,447,705.7243.........	0.1590	4684.4	3.4	6560.4	12.6	4468.8:	1.4:
2,447,705.7360.........	0.3104	4685.3	5.2	6559.4	13.1		
2,447,705.7523.........	0.5220	4684.8	4.8	6565.5	8.4	4466.5	2.7
2,447,705.7639.........	0.6719	4684.7	6.3	6565.5	15.0	4466.1	3.1
2,447,705.7757.........	0.8250	4685.6	6.6	6567.0	18.9	4469.1:	1.7:
2,447,705.7892.........	0.0000	4686.3	10.1	6557.7	30.0		
2,447,705.8031.........	0.1807	4683.9	4.1	6560.5	15.9		
2,447,705.8168.........	0.3583	4682.5	4.5	6564.9:	21.9:	4470.9:	1.8:
2,447,705.8284.........	0.5091	4685.3	4.0	6563.5	7.7	4470.8	2.0
2,447,705.8402.........	0.6615	4686.3	4.4	6549.8:	15.9:	4468.1:	1.5:
2,447,705.8521.........	0.8158	4686.6	8.4	6566.2	31.0		

NOTE.—Values followed by a colon are very uncertain.

© American Astronomical Society • Provided by the NASA Astrophysics Data System

1990ApJ...365..686M

around the compact primary star, and that the erratic eclipse feature in our photometry is probably due to the passage of the darker companion in front of it. The photometry and spectrophotometry indicate that this eclipse is partial, since there is evidence for neither a flat bottom in the light curve nor for a change in color of the energy distribution during minimum light. The emission lines also do not disappear completely. For these reasons we envision that the disk is most likely of a comparable size scale to or slightly larger than the secondary star. In the following subsections, we consider the possibilities that the primary star is either a white dwarf or a neutron star, respectively.

a) *A Cataclysmic Variable System?*

The assumption of a white dwarf primary leads to a class of system known as a cataclysmic variable (CV). There are indeed many known examples with similar orbital periods, although few of these have been observed as classical nova systems. Most of the short-period CVs in fact are either of the SU Ursae Majoris type or of the AM Herculis variety.

The optical spectrum of MS 1603.6+2600 does not resemble a dwarf nova in either outburst or quiescence, showing neither strong emission lines nor broad Balmer absorption lines. These objects are also not particularly strong X-ray sources, with F_x/F_{opt} typically a factor of 5–10 lower than MS 1603.6+2600 (Cordova and Mason 1983).

Many AM Herculis systems have periods close to the 111 minutes we have found for MS 1603.6+2600 (see the review by Liebert and Stockman 1985), and also have high ratios of F_x/F_{opt} compared to most classes of CVs (and comparable to MS 1603.6+2600). However, the emission-line spectra of these magnetic systems generally include strong high-excitation emission due to the X-ray heating. In low accretion states the emission lines can certainly weaken, but in this situation the secondary star should be visible at the redder wavelengths and Zeeman-shifted absorption features from the magnetic white dwarf would possibly be observed. Our observations of Ca II absorption near the systemic velocity and of blueshifted He I absorption lines are consistent instead with formation in a nonmagnetic disk or photosphere, albeit one with an outflowing wind.

If the line spectrum in emission and absorption is attributed to a CV disk and wind, the relative strengths of the helium lines compared to hydrogen may require that the donor gas be helium-rich. We are thus led to consider a third type of model in which the secondary is an evolved helium core (see Hunger, Schonberner, and Rao [1985] for several articles on helium-rich stars). As noted previously, post-asymptotic giant branch subdwarfs and/or objects on the so-called extended horizontal branch can have radii of the appropriate order of magnitude to fit the Roche lobe size. However, the known binaries of this type (the AM CVn systems) actually have much shorter periods of between approximately 20 and 56 minutes. In these the secondary is a very small, fully degenerate helium dwarf. At our longer period we require a larger helium star. With radius less than $\sim 0.2\ R_\odot$ and typical temperatures above 30,000 K, the secondary would compete with the disk as the source of light and line spectrum since it would be of similar size and temperature.

A possible way of accounting for a large enrichment of helium in the accreting gas, but with a trace abundance of hydrogen remaining, might be to hypothesize that the secondary is an evolved nuclear-burning star currently near the end of its main-sequence phase. Since no M dwarf would have time to convert a substantial amount of hydrogen to helium in its convective interior within the lifetime of the universe, this scenario requires the secondary to have had a mass near $\sim 1\ M_\odot$ originally. With CV mass transfer having gone on for a long period of time, this star could have been whittled down in mass by a factor of 5. The system would have to be more than $\sim 10^{10}$ yr old as a halo object, and the current secondary star, part of the original nuclear-burning core, can thus have an arbitrarily helium-rich composition. Since the radius of a star grows only modestly during the main-sequence phase, it is not very likely that Roche lobe overflow would occur first during this phase. It is more likely that the majority of the mass transfer occurs during the (short) phase when the star is growing to be a red giant.

The idea that some CVs might have secondary stars greatly enriched in helium was discussed in detail by Williams and Ferguson (1982), although the CV disk spectra modeled by those authors did not have the strong neutral helium absorption and very weak hydrogen emission characteristic of MS 1603.6+2600.

If this object is a white dwarf accreting from an unusual secondary star, it is reasonable to assume that the optical radiation is dominated by an optically thick accretion disk of size and luminosity similar to those of other CVs with high accretion rate, i.e., dwarf novae in eruption or old novae. Although highly variable, such disks typically have absolute visual magnitudes (M_v) of +4 to +6 (Patterson 1984; Wade 1985). Assuming a mean apparent $V \sim 19.7$, the mean M_v implies a distance of 6–14 kpc or a height above the Galactic plane of 4–10 kpc. If the distance is correct to within even a factor of 4, the binary system would be assignable to the halo population.

b) *A Low-Mass X-Ray Binary?*

The optical spectrum and rather large ratio of X-ray to optical flux both suggest that the accreting primary is a neutron star rather than a white dwarf, and that the appropriate model for MS 1603.6+2600 is that of a low-mass X-ray binary (LMXB) with a low-mass M-type companion. MS 1603.6+2600 does have a ratio F_x/F_{opt} at the extreme low end of the distribution of LMXBs from Van Paradijs (1983). However, eclipsing LMXBs are expected to have low values of F_x/F_{opt} relative to other LMXBs, as the X-ray flux from these systems is often largely the result of scattering from a hot ionized gas above the plane of the accretion disk (an accretion disk corona—see, for example, White and Mason 1985). The direct X-rays from the primary star are absorbed by the disk itself, and only a small fraction of the total flux is scattered into our line of sight by the disk corona. LMXBs do show quite similar line spectra to MS 1603.6+2600, generally characterized by He II, a broad blend of features due to C III and N III at wavelengths around 4640–4650 Å, and weak hydrogen lines. All the lines are relatively weak against the strong continuum (Van Paradijs and Verbunt 1984), as observed here. The higher excitation of the line spectrum relative to most CVs is generally attributable not to unusual abundances in the accreted gas, but to X-ray photoionization. The He I absorption line blueshift suggests that these lines arise in a wind being driven from the central region.

There are many similarities between MS 1603.6+2600 and the LMXB AC 211 in M15 (Ilovaisky 1989; Bailyn, Garcia, and Grindlay 1989; Naylor *et al.* 1988). This system shows a similar optical spectrum with both He II emission and blue-

© American Astronomical Society • Provided by the NASA Astrophysics Data System

1990ApJ...365..686M

shifted He I absorption. AC 211 is considerably brighter in the optical (15–16 magnitude), but presents observational problems of deblending due to its location in a globular cluster. Other points of similarity between the two systems include (i) the optical light curve shows differing shapes as a function of orbital phase on different nights (Aureire *et al.* 1989); (ii) the He II flux is essentially constant with phase (Ilovaisky 1989); (iii) the Hβ line in AC 211 shows a P Cygni profile (Ilovaisky 1989). (While the Hβ profile in MS 1603.6+2600 cannot be described with certainty as P Cygni-like, its large positive velocity relative to Hα seems to indicate such a shape.)

If the LMXB model is correct, the distance to MS 1603.6+2600 is very uncertain but could be very large. There are several lines of argument which indicate this. The negative orbit-averaged heliocentric radial velocity of the system in both Ca II and He II indicate a location on the far side of the Galactic center if the object shares in the disk rotation. Also, assuming the system to be a typical LMXB with $M_v = 1.2 \pm 1.0$ (Van Paradijs 1983) would put the system at a distance of $\sim$30–80 kpc, i.e. $\sim$22–58 kpc above the Galactic plane. Galactic reddening in this direction is small ($E_{B-V} \leq 0.06$, Burstein and Heiles 1982) and will not significantly reduce this distance estimate. The similarity to AC 211 also suggests that the distance may be large. Cowley *et al.* (1989) note that eclipsing LMXBs have X-ray luminosities of $\sim 10^{36}$ ergs cm^{-2} s^{-1}, which would also put MS 1603.6+2600 at a distance of 80 kpc. Alternatively, MS 1603.6+2600 may be an example of the underluminous LMXB suggested by Chevalier and Ilovaisky (1987).

One of the simplest ways to determine the correct model for MS 1603.6+2600 will be to acquire further long-term X-ray data. *ROSAT* observations have been scheduled, and will almost certainly determine whether the white dwarf or LMXB model is correct. These data will also help determine the intrinsic X-ray luminosity and hence the distance to this source.

If it is a LMXB, the origin of MS 1603.6+2600 is unclear. The current theory for the origin of LMXB systems in the Galactic plane suggests that they are the result of supernovae in binaries that went through a common envelope phase of evolution (van den Heuvel 1983). Such systems can have large space velocities even when the binary remains bound, and so MS 1603.6+2600 could have reached its current position well away from the Galactic plane in a few times 10^8 yr. Alternatively, LMXBs in globular clusters may be formed by capture of a secondary star by an already formed neutron star in the dense core of the globular (Fabian, Pringle, and Rees 1975). Some of these systems will be ejected from the globular cluster (Statler, Ostriker, and Cohn 1987) and could hence be the progenitor of MS 1603.6+2600.

If confirmed as a LMXB, MS 1603.6+2600 will be the first in the period range 1–2 hr. The absence of LMXB systems with periods matching the CV SU UMa and AM Her systems has been commented on by several authors (e.g., White and Mason 1985), although no selection effect against such systems is known.

V. CONCLUSIONS

MS 1603.6+2600 is an eclipsing X-ray selected binary system at high Galactic latitude. It has optical magnitude $R \sim 19.4$ and period 111 minutes. Differential photometry shows the light curve varies from night to night—sometimes showing clear eclipses, and sometimes not. Its spectra show weak emission lines of He II and the Balmer series together with He I and Ca II absorption lines. The emission-line flux is approximately independent of orbital phase. The He I absorption lines are blueshifted relative to the emission lines and the Ca II absorption.

A model involving a white dwarf primary would probably require a helium-rich secondary to explain the He II to Hα ratio. Spectroscopic similarities with the LMXB system AC 211 in M15 make it more likely that there is a neutron star primary. If the object has an optical luminosity in the range seen for LMXBs, its distance must be 30–80 kpc. Such a distance would also match the X-ray luminosity seen in eclipsing LMXBs.

We would like to thank Rex Saffer for advice on radial velocity standards and heliocentric corrections, and Buell Jannuzi for communicating his linear polarization measurements in advance of publication. We are also grateful to the referee for a thorough review which improved the presentation of the paper. S. L. M. is funded through NASA contract NAS5-30101. J. L. acknowledges with pleasure the support and hospitality of the Observatories of the Carnegie Institution of Washington for his sabbatical stay. J. S. acknowledges support through NSF grant AST 8715983 and NASA grant NAG 5-1224. Work on the EMSS at CfA is supported by NASA grant NAS 8-30751 and the Scholarly Studies Program grant SS88-03-87.

REFERENCES

Auriere, M., Ilovaisky, S. A., Koch-Miramond, L., Chevalier, C., and Cordoni, J. 1989, preprint.
Baars, J. W. M., Genzel, R., Pauliny-Toth, I. T. U., and Witzel, A. 1977, *Astr. Ap.*, **61**, 99.
Bailyn, C. D., Garcia, M. R., and Grindlay, J. E. 1989, *Ap. J.*, **344**, 786.
Burstein, D., and Heiles, C. 1982, *A.J.*, **87**, 1165.
Chevalier, C., and Ilovaisky, S. A. 1987, *Astr. Ap.*, **172**, 167.
Cowley, A. P., Schmidtke, P. C., Crampton, D., and Hutchings, J. B. 1989, preprint.
Cordova, F. A., and Mason, K. O. 1983, in *Accretion-Driven Stellar X-ray Sources*, ed. W. H. G. Lewin and E. P. J. van den Heuvel (Cambridge: Cambridge University Press), p. 147.
Fabian, A. C., Pringle, J. E., and Rees, M. 1975, *M.N.R.A.S.*, **172**, 15P.
Fleming, T. A., Gioia, I. M., and Maccacaro, T. 1989, *Ap. J.*, **340**, 1011.
Gioia, I. M., Maccacaro, T., Schild, R. E., Wolter, A., Stocke, J. T., Morris, S. L., and Henry, J. P. 1990, *Ap. J. Suppl.*, **72**, 567.
Hunger, K., Schonberner, D., and Rao, N. 1985, ed. *Hydrogen Deficient Stars and Related Objects* (Dordrecht: Reidel).
Ilovaisky, S. A. 1989, preprint.
Liebert, J., and Stockman, H. S. 1985, in *Cataclysmic Variables and Low Mass X-ray Binaries*, ed. J. Patterson and D. Q. Lamb (Dordrecht: Reidel), p. 179.
Maccacaro, T., Gioia, I. M., Wolter, A., Zamorani, G., and Stocke, J. 1988, *Ap. J.*, **326**, 680.
Morris, S. L., Schmidt, G. D., Liebert, J., Stocke, J., Gioia, I. M., and Maccacaro, T. 1987, *Ap. J.*, **314**, 641.
Naylor, T., Charles, P. A., Drew, J. E., and Hassall, B. J. M. 1988, *M.N.R.A.S.*, **233**, 285.
Patterson, J. 1984, *Ap. J. Suppl.*, **54**, 443.
Peterson, R. C., Olszewski, E. W., and Aaronson, M. 1986, *Ap. J.*, **307**, 139.
Pringle, J. E. 1985, in *Interacting Binary Systems*, ed. J. E. Pringle and R. A. Wade (Cambridge: Cambridge University Press), p. 9.
Raymond, J. C., and Smith, B. W. 1977, *Ap. J. Suppl.*, **35**, 419.

© American Astronomical Society • Provided by the NASA Astrophysics Data System

1990ApJ...365..686M

Statler, T., Ostriker, J. P., and Cohn, H. 1987, *Ap. J.*, **316**, 626.
Stocke, J. T., Morris, S. L., Gioia, I., Maccacaro, T., Schild, R. E., and Wolter, A. 1990*a*, *Ap. J.*, **348**, 141.
Stocke, J. T., Morris, S. L., Fleming, T. A., Gioia, I., Maccacaro, T., Schild, R. E., Wolter, A., and Henry, J. P. 1990*b*, in preparation.
van den Heuvel, E. P. J. 1983, in *Accretion-Driven Stellar X-Ray Sources*, ed. W. H. G. Lewin and E. P. J. van den Heuvel (Cambridge: Cambridge University Press), p. 189.
Van Paradijs, J. 1983, in *Accretion-Driven Stellar X-Ray Sources*, ed. W. H. G. Lewin and E. P. J. van den Heuvel (Cambridge: Cambridge University Press), p. 189.
Van Paradijs, J., and Verbunt, F. 1984, in *High-Energy Transients in Astrophysics*, ed. S. E. Woosley (NY: AIP), p. 49.
Wade, R. A. 1985, in *Interacting Binaries*, ed. P. P. Eggleton and J. E. Pringle (Dordrecht: Reidel), p. 289.
White, N. E., and Mason, K. O. 1985, *Space Sci. Rev.*, **40**, 167.
Williams, R. E., and Ferguson, D. H. 1982, *Ap. J.*, **257**, 672.

SIMON L. MORRIS: The Observatories of the Carnegie Institution of Washington, 813 Santa Barbara Street, Pasadena, CA 91101

JAMES LIEBERT: Steward Observatory, University of Arizona, Tucson, AZ 85721

ISABELLA M. GIOIA, RUDY E. SCHILD, and ANNA WOLTER: Harvard Smithsonian Center for Astrophysics, 60 Garden St., Cambridge, MA 02138

JOHN T. STOCKE: Center for Astrophysics and Space Astronomy, University of Colorado, Campus Box 391, Boulder, CO 80309

© American Astronomical Society • Provided by the NASA Astrophysics Data System